OL | Organic Letters

pubs.acs.org/OrgLett Letter

Accelerated Reactivity Mechanism and Interpretable Machine Learning Model of *N*-Sulfonylimines toward Fast Multicomponent Reactions

Krupal P. Jethava,[@] Jonathan Fine,[@] Yingqi Chen, Ahad Hossain, and Gaurav Chopra*

Cite This: https://dx.doi.org/10.1021/acs.orglett.0c03083 Read Online

ACCESS | Metrics & More | Article Recommendations | Supporting Information

ABSTRACT: We introduce chemical reactivity flowcharts to help chemists interpret reaction outcomes using statistically robust machine learning models trained on a small number of reactions. We developed fast *N*-sulfonylimine multicomponent reactions for understanding reactivity and to generate training data. Accelerated reactivity mechanisms were investigated using density functional theory. Intuitive chemical features learned by the model accurately predicted heterogeneous reactivity of *N*-sulfonylimine with different carboxylic acids. Validation of the predictions shows that reaction outcome interpretation is useful for human chemists.

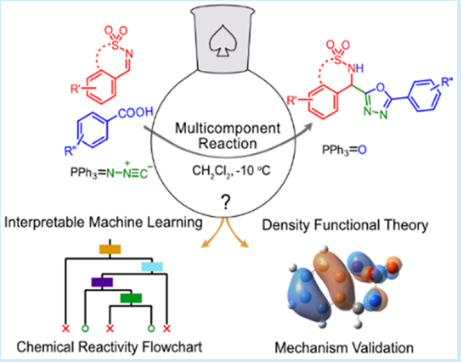

Computer-assisted organic chemistry has huge potential for predicting chemical reaction conditions and for automating synthetic chemistry.[1−3] In recent years, machine learning (ML)-based approaches have been successfully applied to screen libraries of druglike molecules,[4,5] for quantitative structure−activity relationships (QSARs),[6] for retrosynthetic planning,[7−12] for reaction condition prediction,[13] and for reaction prediction.[12] Reactivity prediction is a hard problem that requires specific experimental data sets to train ML models.[14,15] Traditionally, creating such experimental databases requires a large number of manual experiments to check the feasibility of available starting materials to determine if it reacts together. It is important to note that most ML methods use existing databases and use only successful reactions published in the literature as reporting of unsuccessful reaction is scarcely available. Thus, for a specific case study through the careful training of ML models using both successful and unsuccessful reaction data, it is possible to train on smaller data sets to test specific synthetic objectives. Recently, smaller data sets were used for prediction but without experimental validation of regiostereoisomers, site stereoisomers, diastereoisomers in Diels−Alder reaction,[16] and radical C−H functionalization of heterocycles.[17] ML models are helpful in building a chemical library that is otherwise tedious to explore by screening each reaction to check substrate feasibility under certain reaction conditions. To date, there is limited literature precedence for prospective validation of desired chemical reactions and interpreting its reactivity using ML methods.[18,19] We provide the first report, to the best of our knowledge, of a fast and one-pot multicomponent reaction to explore heterogeneous reactivity of *N*-sulfonylimines by training a human interpretable ML model that identifies chemical patterns of reactivity to predict and test the reactivity of new substrates in the multicomponent reactions prospectively.

We selected *N*-sulfonylimines as our model substrate because *N*-sulfonylimines are one of the important synthons in organic chemistry that is used for a variety of chemical transformations. *N*-Sulfonylimine is a good source of an electrophilic carbon for radical[20] and nucleophilic addition[21,22] reactions. Several reports have described *N*-sulfonylimine reactions in which the reactivity of a carbon−nitrogen double bond is exploited.[23] Notably, sulfamidate,[24] a cyclic *N*-sulfonylimine, has been used to prepare interesting heterocyclic scaffolds. Sulfamidate is transformed into a fused heterocycle using a Michael addition,[25] cycloaddition,[26−31] arylation,[32−34] alkenylation,[35−37] or alkynylation[35] strategy by leveraging the electrophilicity of sulfamidate (Scheme 1).

However, among the reported synthetic strategies, construction of a direct C−C bond between the imine carbon and the (het)aromatic partner is underrepresented in the literature. Specifically, a synthetic strategy for the direct C−C bond

Received: September 14, 2020

https://dx.doi.org/10.1021/acs.orglett.0c03083
Org. Lett. XXXX, XXX, XXX−XXX

Scheme 1. Strategy for Exploring *N*-Sulfonylimine Reactivity toward Multicomponent Reactions

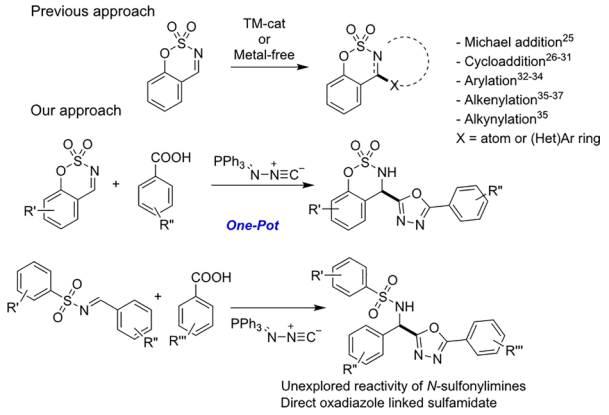

linkage between sulfamidate and oxadiazole has not been explored to date. The oxadiazole scaffold is a unique presence in many biologically active compounds[38−40] and pharmaceutical agents and is a privileged scaffold in material science (Figure 1).[41] Therefore, sulfamidate-linked 1,3,4-oxadiazole could be useful for the chemical library design of new druglike scaffolds.

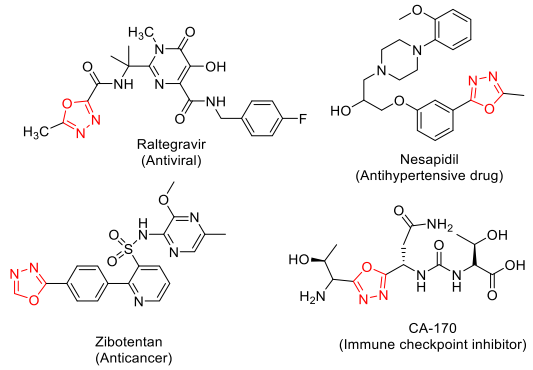

Figure 1. Compounds with 1,3,4-oxadiazole in medicinal chemistry.

Multicomponent reactions (MCRs) have attracted medicinal chemists to prepare chemical libraries of biologically important molecules and drugs[42] in a rapid manner using two or more building blocks.[43−46] However, MCRs are highly dependent on the reactivity of starting materials as well as the presence of the solvents, catalysts, concentrations, and equivalents of reagents being used.[42] The understanding of the chemical reactivity of the starting materials for a particular MCR would be useful for identifying specific starting materials for reaction outcomes. A machine learning model for interpreting chemical reactivity and reaction outcome can suggest a type of starting material to be used successfully to obtain the desired product, thereby reducing the waste of valuable reagents, time, and effort. Keeping this in mind, we developed a MCR of cyclic or acyclic *N*-sulfonylimine with carboxylic acid-containing starting materials to generate training data and understand chemical reactivity. Previously, Ramazani et al.[47] and Yudin et al.[48,49] individually reported a four-component reaction yielding a 1,3,4-oxadiazole scaffold using aromatic reactants and peptides, respectively, using *N*-isocyanoimino triphenylphosphorane (PINC) as a reaction partner. In the previous studies, the imine was generated *in situ* from the amine and aldehyde. It is noteworthy that *in situ* formation of imines is not always favorable for several reasons. (i) A reaction could be partially reversible. (ii) The product formed could be unstable under certain reaction conditions.[50] (iii) Imine formation is highly dependent upon its starting materials, an aldehyde and an amine, limiting the use of the previous approaches when we want to use sulfonamides. Alternatively, aryl chloride[51] can be used instead of carboxylic acids but has a limited substrate scope. To address these issues, we provide the first report of using *N*-sulfonylimine as a substrate for a fast and single-step approach to synthesize sulfamidate-embedded 1,3,4-oxadiazole using MCR.

We started our investigation with the idea that several types of cyclic *N*-sulfonylimines, acyclic *N*-sulfonylimines, and aromatic imines are known in the literature and easily synthesized. To determine the pattern of electrophilicity of various imines with carboxylic acids, we used Fukui reaction parameters calculated using density functional theory (DFT)[52] and identified the most suitable imines using the electrophilicity of the carbon atom (Figure S1). Both cyclic and acyclic *N*-sulfonylimines are highly susceptible to the nucleophilic attack of carboxylic acids according to the calculation. Therefore, we started our investigation using the model substrate cyclic *N*-sulfonylimine (sulfamidate) **1a**, which can be easily synthesized from substituted salicylaldehydes. We initially selected benzoic acid as the second reaction partner because of its moderate nucleophilic tendency (Figure S1) and because it would help with the selection of optimized conditions for the future use of a chemically diverse range of carboxylic acids. In addition, the synthesis of other derivatives with the optimized condition would serve as a training data set to develop a robust bootstrapped machine learning model that is human interpretable to guide prospective synthetic experiments using fast MCRs of *N*-sulfonylimines.

Initially, we performed an optimization study using sulfamidate (**1a**) and benzoic acid (**2a**) to form the desired product **3a** (Table 1 for Scheme 2). The optimized reaction condition was obtained when dichloromethane (DCM) was added at the end after taking all starting materials at −10 °C (see the Supporting Information for Reaction condition optimization study).

Table 1. Optimization of the Synthesis of 1,3,4-Oxadiazole[a]

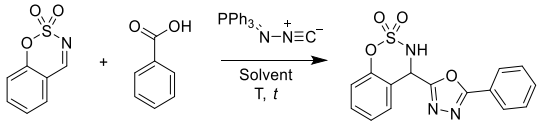

1a 2a 3a

entry	solvent(s)	T (°C)	t (min)	yield (%)[e]
1[b]	DCE:MeCN	50	120	trace
2	DCE	25	120	trace
3	DCM	25	120	<5
4	DCM	25	30−120	<5
5	DCM	Ice-bath	5−30	25
6[c]	DCM	−10	5	40
7[d]	DCM	−10	5	67

[a]Reactions at a 0.1 mmol scale. DCE, dichloroethane; MeCN, acetonitrile. [b]Reaction condition followed as per the literature.[48] [c]Benzoic acid added at the end. [d]All solid components were taken together, and solvent was added at the end. [e]Isolated yield.

https://dx.doi.org/10.1021/acs.orglett.0c03083
Org. Lett. XXXX, XXX, XXX−XXX

Scheme 2. Synthesis of 1,3,4-Oxadiazole Using Cyclic and Acyclic Imine with Benzoic Acid with Optimized Reaction Conditions

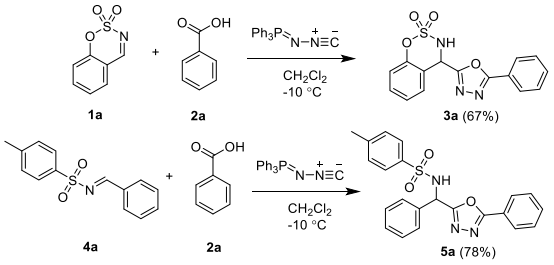

Next, we applied the optimized reaction condition to the acyclic *N*-sulfonylimine selected using DFT calculations (Figure S1) as it was the second most reactive imine. Also, we sought to develop a one-pot strategy for preparing 1,3,4-oxadiazole-linked sulfonamide compared to the four-step synthesis reported previously.[53] Interestingly, when acyclic *N*-sulfonylimine (**4a**) was reacted with benzoic acid (**2a**) under optimized conditions, the reaction afforded the desired product (**5a**) in good yield (Scheme 2), but with a longer reaction time (10 min) for the complete conversion compared to that of sulfamidate (<5 min). This led us to investigate the mechanism and the energy profile of plausible intermediates and transition states formed in this reaction.

To gain mechanistic insight into the chemical reactions, we used DFT with a polarized continuum model for DCM solvation at −10 °C to identify transition states and intermediates for acyclic (Figure S2) and cyclic *N*-sulfonylimines (Figure S3). In the proposed mechanism, the nucleophilic attack by the negatively charged carbon atom of PINC on the electrophilic center of *N*-sulfonylimine yields Intermediate-1. The subsequent Intermediate-2 is formed by a nucleophilic attack of benzoic acid. Next, intramolecular cyclization at the carbonyl carbon, formation of the oxazaphosphetane intermediate, and subsequent removal of triphenylphosphine oxide yield the desired 1,3,4-oxadiazole-containing product (see Figures S2−S7 and Tables S1, S1a, S1b, and S2). All files and animation are available at https://chopralab.github.io/n_sulfonylimine_reactions/.

The energy profile in the proposed mechanism also suggests why cyclic *N*-sulfonylimine would be faster than the acyclic *N*-sulfonylimine. The first half of the reaction mechanism, until formation of Intermediate-2, is dependent on the chemistry of acyclic or cyclic *N*-sulfonylimines (Figures S2 and S3). In both cases, the rate-limiting step is the attack of the PINC reagent on the *N*-sulfonylimine with changes in free energy ($\Delta G_{barrier}$) of 16.3 and 12.6 kcal/mol for the acyclic and cyclic *N*-sulfonylimines, respectively. This suggests that both reactions will occur quickly, and it is expected that the cyclic *N*-sulfonylimine would be faster than the acyclic *N*-sulfonylimine, which has been shown experimentally.

Next, using the optimized conditions, we started investigating various sulfamidates and carboxylic acid derivatives. The reaction of the diethylamine-containing sulfamidate (**1b**) with benzoic acid (**2a**) afforded the desired product **3b** in 46% yield. The reaction of sulfamidate **1b** with *p*-toluic acid (**2b**) also formed product **3c** but in low yield (17%). In addition, reaction of methoxy-substituted sulfamidate **1c** with benzoic acid (**2a**) formed expected product **3d** in moderate yield (52%). However, naphthyl sulfamidate (**1d**) did not react effectively, giving 1,3,4-oxadiazole **3e** in poor yield. Notably, bromo derivatives of sulfamidate **1e** with benzoic acid (**2a**) did not afford the desired product (**3f**). Nonetheless, when sulfamidate **1c** was reacted with pyridine carboxylic acid **2c**, it formed the expected product with an inseparable isomer in poor yield. In addition, 4-hydroxybenzoic acid (**2d**) did not react with sulfamidate **1c** to form the desired product **3h**. Next, we also sought to study the reactivity of other carboxylic acids with sulfamidates. Therefore, apart from the products shown in Scheme 3, we also attempted other reactions to study the

Scheme 3. Substrate Scope for Representative Cyclic *N*-Sulfonyl-imine with Various Carboxylic Acids Used as Training Data

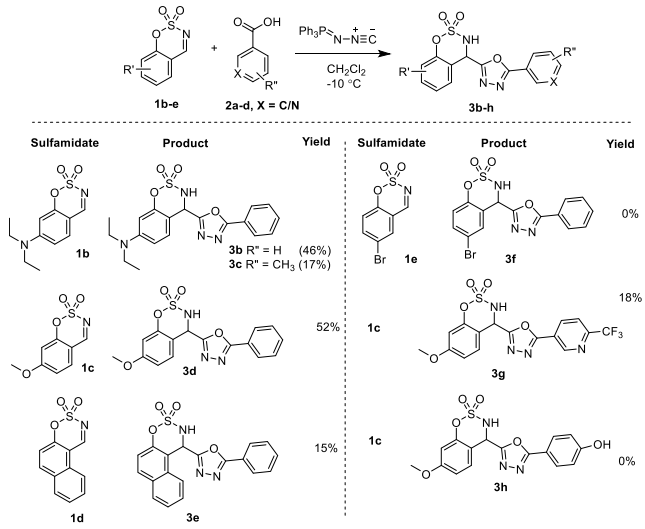

reactivity of sulfamidate with other carboxylic acids (see Scheme S1). For example, difluoro arylacetic acid, pyrimidine-2-carboxylic acid, terephthalic acid, etc., did not react well with sulfamidates.

The heterogeneous reactivity of sulfamidates made us intrigued to study the reactivity of acyclic *N*-sulfonylimines with carboxylic acids after the successful model reaction shown in Scheme 2. As shown in Scheme 4, acyclic *N*-sulfonylimine substrates were reacted with benzoic acids. Unlike halogenated sulfamidates, the reaction of halogenated acyclic *N*-sulfonylimine **4b** reacted well with benzoic acid (**2a**) and 4-bromo-3-methyl benzoic acid (**2e**), giving the desired products **5b** and

Scheme 4. Substrate Scope for Acyclic *N*-Sulfonylimine with Carboxylic Acids Used as Training Data

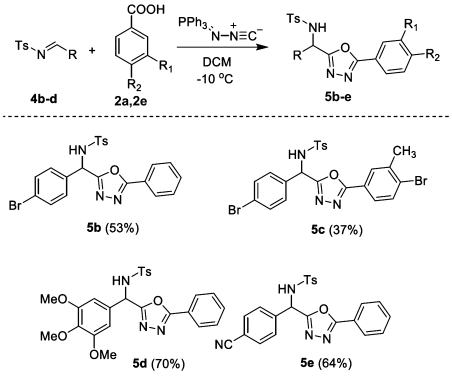

https://dx.doi.org/10.1021/acs.orglett.0c03083
Org. Lett. XXXX, XXX, XXX−XXX

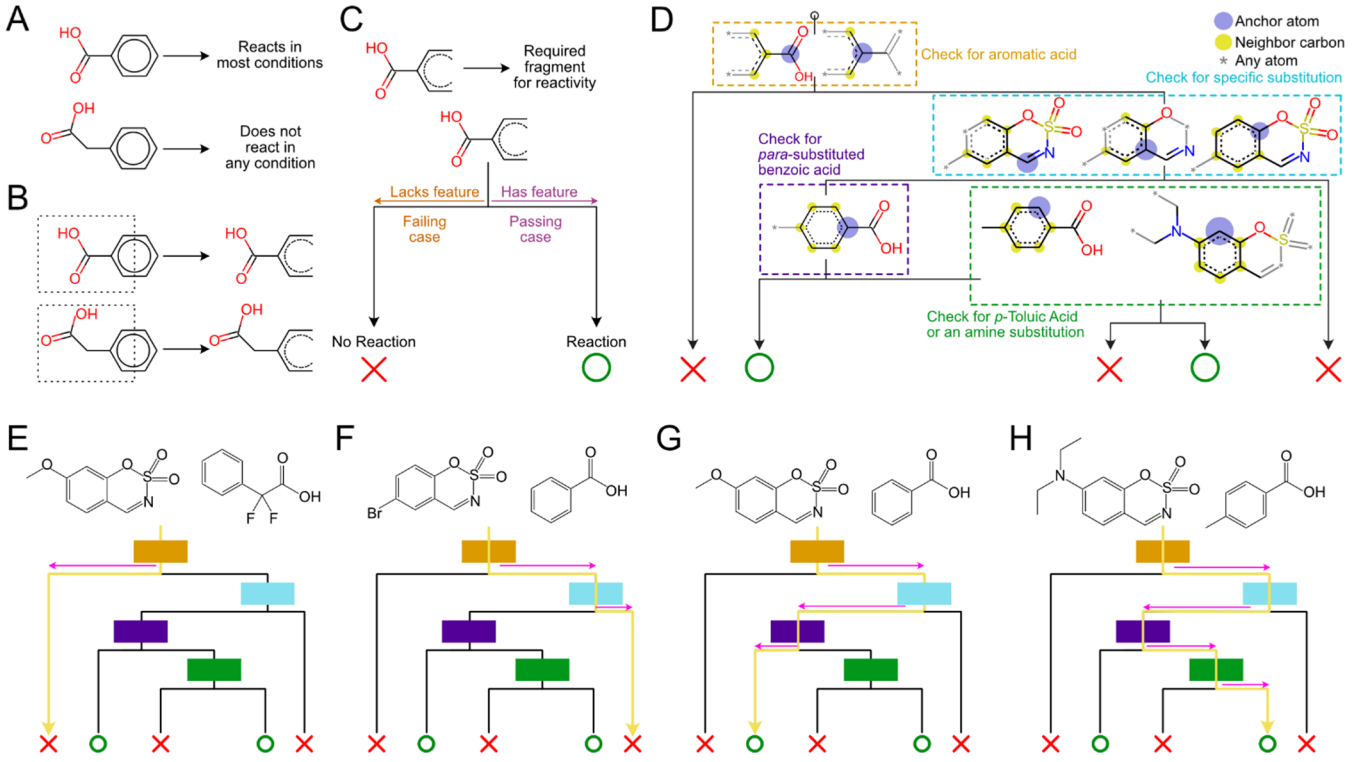

Figure 2. Chemical reactivity flowchart. Decision tree model for the substrate scope of the reaction between imine and acid. (A–C) Pictorial explanation of how the model assigns rules for predicting reactivity. (D) Final bootstrapped model trained on all data with details for each rule shown in colored boxes. (E–H) Examples of each of these rules using the training data. Box colors represent features shown in panel D, and the yellow line of the flowchart shows the reaction outcome based on chemical features.

5c in 53% and 37% yields, respectively. In addition, the syntheses of **5d** and **5e** were achieved successfully using trimethoxy-substituted *N*-sulfonylimine (**4c**) and 4-cyano-substituted *N*-sulfonylimine (**4d**), respectively, and they were well tolerated to afford the desired products **5d** and **5e**, respectively (70% and 64% yields, respectively).

The heterogeneous reactivity of cyclic and acyclic *N*-sulfonylimines motivated us to develop a machine learning model using the successful and unsuccessful reactions. We trained decision tree[54] models using the extended connectivity fingerprints (ECFP)[55] of the carboxylic acids and *N*-sulfonylimines determined separately. For a fingerprint radius of 0–3, no major bit collisions were observed. Each reaction is assigned a reaction ID and a binary condition ("Worked" in Table S3) to represent whether a reaction occurs between the *N*-sulfonylimine and carboxylic acid. The goal of the decision tree models is to predict the "Worked" response using the fingerprints. Due to the limited amount of reactions available for training (20 reactions), multiple fingerprint features may represent the same split in the decision. To address this issue, the validation of the decision trees was performed 1000 times to sample the different possible models that can be created for a given fingerprint radius (shown in Figures S8 and S9). We used bootstrapping of several decision tree models to ensure the robustness of our model for predicting prospective experimental outcomes (see the Supporting Information, figures and tables for bootstrapped decision tree models, for details that include an introduction of the machine learning method used in this work). A Cohen κ statistic of 0.706 was obtained with an ECFP fingerprint radius of 3 for the final model, suggesting strong intermodel reliability on limited training data (20 reactions).[56,57] This methodology yields the chemical reactivity flowcharts with features shown in Figure 2A–D that can be used to investigate additional reactions to ensure that the model is predictive while maintaining interpretability.

The final model's chemical reactivity flowchart shown in Figure 2D is used to interpret and evaluate the substrate scope of the reaction given the limited number of reactions available for training. The first decision of the model is a check for a carboxylic acid group adjacent to an aromatic ring where the lack of this feature leads to a prediction of no reaction (an example of a failing case when the feature is lacking is shown in Figure 2E). Next, the model checks for the substitution at position 6 of the cyclic imine where a substitution at this position results in the prediction of no reaction (example of a feature passing case given in Figure 2F). Next, the model checks for the presence of a substitution at the *para* position of the carboxylic acid where the lack of this feature results in the prediction that a reaction will occur. An example of this feature failing case is given in Figure 2G. Note that any substitution other than a *para* substitution, including heteroaromatics, will result in the failing case. Finally, the model checks for a diethylamine substitution at position 7 of sulfonylimine or whether the carboxylic acid is *p*-toluic acid. All decisions made by the ML model were highly confident except for the final decision (green box in Figure 2H where the only reaction passing this condition is shown). This decision is supported by only a *p*-toluic acid or an amine substitution. Therefore, the model is unable to distinguish between specific features that resulted in a successful reaction. To elucidate chemistry at this step, we tested the reaction between **1c** (*N*-sulfonylimine without an amine substitution) and **2b** (*p*-toluic acid) and noted that the reaction occurred. Conversely, the reaction

https://dx.doi.org/10.1021/acs.orglett.0c03083
Org. Lett. XXXX, XXX, XXX–XXX

between **1b** (*N*-sulfonylimine with an amine substitution) and **2d** (4-hydroxy benzoic acid) did not occur. These results show that the final decision should check for *p*-toluic acid and not an amine substitution. Finally, we tested **2d** with the acyclic *N*-sulfonylimine **4a** to see if this rule applied to acyclic *N*-sulfonylimines and noted that the reaction does occur. These reactions are shown in Scheme 5 and show how our ML

Scheme 5. Reactions Performed to Test the ML Model

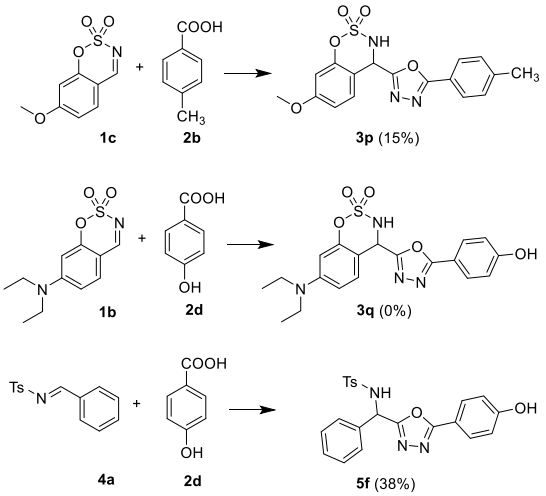

strategy can be used to interpret the reactions by MCR similar to a human chemist. These reactions elucidate that the final decision of the model is supported by two different features to predict reaction outcome. The additional reactions clarify this rule as they show that a *p*-methyl substitution in benzoic acid is responsible for reactivity and that a *p*-hydroxy substitution leads to decreased reactivity for cyclic *N*-sulfonylimine. It also suggests that acyclic *N*-sulfonylimines are more reactive than the cyclic forms as they also react with *p*-hydroxy benzoic acid. Therefore, the use of bootstrapping is essential for developing reliable models for smaller data sets, and the judicious use of decision tree models on positive and negative reactions will help human and machine chemists interpret reaction outcomes.

In summary, we have developed a fast MCR of acyclic or cyclic *N*-sulfonylimines that was used as a representative reaction type to develop ML models for predicting reaction outcomes in a blind prospective manner.[58] The fast and peculiar reactivity mechanism of *N*-sulfonylimines was explained using DFT calculation to understand the critical role of transition states and intermediates. Bootstrapped decision tree-based ML models resulted in a chemical reactivity flowchart that explained the choices made by the model to predict reaction outcomes. The human interpretable ML approach can be extended to explore any MCR or any chemical reaction used to synthesize a library of compounds in a quick and efficient manner. In addition, the generated chemical library could be expanded by Suzuki coupling,[51] ring opening through -SO_2 extrusion,[26] or tosyl group removal[53] using known reaction conditions. This work provides a framework for developing fast MCRs, understanding the underlying reaction mechanism, and identifying chemical features for predicting the reactivity of components that results in successful reactions to save valuable time for chemists to avoid chasing dead-end leads.

■ ASSOCIATED CONTENT

Supporting Information

The Supporting Information is available free of charge at https://pubs.acs.org/doi/10.1021/acs.orglett.0c03083.

Copies of ^{1}H and ^{13}C NMR spectra for all new compounds, supporting text for the reaction mechanism, supporting text for the bootstrapping of decision tree models, and experimental section for synthesis for validation of the machine learning model (PDF)

■ AUTHOR INFORMATION

Corresponding Author

Gaurav Chopra − *Department of Chemistry, Purdue Institute for Drug Discovery, Purdue Institute for Integrative Neuroscience, Purdue Institute for Inflammation, Immunology and Infectious Disease, Purdue Center for Cancer Research, and Purdue University Integrative Data Science Initiative, Purdue University, West Lafayette, Indiana 47907, United States;* orcid.org/0000-0003-0942-7898; Email: gchopra@purdue.edu

Authors

Krupal P. Jethava − *Department of Chemistry, Purdue University, West Lafayette, Indiana 47907, United States;* orcid.org/0000-0002-4440-3333

Jonathan Fine − *Department of Chemistry, Purdue University, West Lafayette, Indiana 47907, United States*

Yingqi Chen − *Department of Chemistry, Purdue University, West Lafayette, Indiana 47907, United States*

Ahad Hossain − *Department of Chemistry, Purdue University, West Lafayette, Indiana 47907, United States*

Complete contact information is available at: https://pubs.acs.org/10.1021/acs.orglett.0c03083

Author Contributions

[@]K.P.J. and J.F. contributed equally to this work.

Notes

The authors declare no competing financial interest.

■ ACKNOWLEDGMENTS

This work was supported, in part, by a Purdue University start-up package from the Department of Chemistry at Purdue University, a Ralph W. and Grace M. Showalter Research Trust award, the Integrative Data Science Initiative award, the Jim and Diann Robbers Cancer Research Grant for New Investigators award, and NIH NCATS ASPIRE Design Challenge awards to G.C. and a Lynn Fellowship to J.F. Additional support, in part, by the NSF I/UCRC Center for Bioanalytical Metrology (Award 1916691), a NCATS Clinical and Translational Sciences Award from the Indiana Clinical and Translational Sciences Institute (UL1TR002529), and the Purdue University Center for Cancer Research (NIH Grant P30 CA023168) is also acknowledged. ChemAxon software support is acknowledged.

■ REFERENCES

(1) Corey, E. J.; Wipke, W. T. Computer-Assisted Design of Complex Organic Syntheses Published by: American Association for the Advancement of Science Stable URL: Http://Www.Jstor.Org/Stable/1727162 Digitize, Preserve and Extend Access to Science of New Computer-Assisted Design of C. *Science (Washington, DC, U. S.)* **1969**, *166* (3902), 178−192.

(2) Gao, H.; Struble, T. J.; Coley, C. W.; Wang, Y.; Green, W. H.; Jensen, K. F. Using Machine Learning to Predict Suitable Conditions for Organic Reactions. *ACS Cent. Sci.* **2018**, *4* (11), 1465−1476.
(3) Granda, J. M.; Donina, L.; Dragone, V.; Long, D. L.; Cronin, L. Controlling an Organic Synthesis Robot with Machine Learning to Search for New Reactivity. *Nature* **2018**, *559* (7714), 377−381.
(4) Lavecchia, A. Machine-Learning Approaches in Drug Discovery: Methods and Applications. *Drug Discovery Today* **2015**, *20* (3), 318−331.
(5) Rodríguez-Pérez, R.; Miyao, T.; Jasial, S.; Vogt, M.; Bajorath, J. Prediction of Compound Profiling Matrices Using Machine Learning. *ACS Omega* **2018**, *3* (4), 4713−4723.
(6) Ma, J.; Sheridan, R. P.; Liaw, A.; Dahl, G. E.; Svetnik, V. Deep Neural Nets as a Method for Quantitative Structure-Activity Relationships. *J. Chem. Inf. Model.* **2015**, *55* (2), 263−274.
(7) Badowski, T.; Molga, K.; Grzybowski, B. A. Selection of Cost-Effective yet Chemically Diverse Pathways from the Networks of Computer-Generated Retrosynthetic Plans. *Chem. Sci.* **2019**, *10* (17), 4640−4651.
(8) Fooshee, D.; Mood, A.; Gutman, E.; Tavakoli, M.; Urban, G.; Liu, F.; Huynh, N.; Van Vranken, D.; Baldi, P. Deep Learning for Chemical Reaction Prediction. *Mol. Syst. Des. Eng.* **2018**, *3* (3), 442−452.
(9) Szymkuć, S.; Gajewska, E. P.; Klucznik, T.; Molga, K.; Dittwald, P.; Startek, M.; Bajczyk, M.; Grzybowski, B. A. Computer-Assisted Synthetic Planning: The End of the Beginning. *Angew. Chem., Int. Ed.* **2016**, *55*, 5904−5937.
(10) Liu, B.; Ramsundar, B.; Kawthekar, P.; Shi, J.; Gomes, J.; Luu Nguyen, Q.; Ho, S.; Sloane, J.; Wender, P.; Pande, V. Retrosynthetic Reaction Prediction Using Neural Sequence-to-Sequence Models. *ACS Cent. Sci.* **2017**, *3* (10), 1103−1113.
(11) Klucznik, T.; Mikulak-Klucznik, B.; Mccormack, M. P.; Mrksich, M.; Trice, S. L. J.; Grzybowski, B. A.; et al. Efficient Syntheses of Diverse, Medicinally Relevant Targets Planned by Computer and Executed in the Laboratory. *Chem* **2018**, *4*, 522−532.
(12) Wei, J. N.; Duvenaud, D.; Aspuru-Guzik, A. Neural Networks for the Prediction of Organic Chemistry Reactions. *ACS Cent. Sci.* **2016**, *2* (10), 725−732.
(13) Gao, H.; Struble, T. J.; Coley, C. W.; Wang, Y.; Green, W. H.; Jensen, K. F. Using Machine Learning to Predict Suitable Conditions for Organic Reactions. *ACS Cent. Sci.* **2018**, *4* (11), 1465−1476.
(14) Segler, M. H. S.; Waller, M. P. Neural-Symbolic Machine Learning for Retrosynthesis and Reaction Prediction. *Chem. - Eur. J.* **2017**, *23* (25), 5966−5971.
(15) Coley, C. W.; Green, W. H.; Jensen, K. F. Machine Learning in Computer-Aided Synthesis Planning. *Acc. Chem. Res.* **2018**, *51* (5), 1281−1289.
(16) Beker, W.; Gajewska, E. P.; Badowski, T.; Grzybowski, B. A. Prediction of Major Regio-, Site-, and Diastereoisomers in Diels−Alder Reactions by Using Machine-Learning: The Importance of Physically Meaningful Descriptors. *Angew. Chem., Int. Ed.* **2019**, *58* (14), 4515−4519.
(17) Li, X.; Zhang, S.; Xu, L.; Hong, X. Predicting Regioselectivity in Radical C−H Functionalization of Heterocycles through Machine Learning. *Angew. Chem., Int. Ed.* **2020**, *59* (32), 13253−13259.
(18) Ahneman, D. T.; Estrada, J. G.; Lin, S.; Dreher, S. D.; Doyle, A. G. Predicting Reaction Performance in C−N Cross-Coupling Using Machine Learning. *Science (Washington, DC, U. S.)* **2018**, *360* (6385), 186−190.
(19) Nielsen, M. K.; Ahneman, D. T.; Riera, O.; Doyle, A. G. Deoxyfluorination with Sulfonyl Fluorides: Navigating Reaction Space with Machine Learning. *J. Am. Chem. Soc.* **2018**, *140* (15), 5004−5008.
(20) Miyabe, H.; Ueda, M.; Naito, T. N-Sulfonylimines as an Excellent Acceptor for Intermolecular Radical Reactions. *Chem. Commun.* **2000**, No. 20, 2059−2060.
(21) Izquierdo, J.; Pericàs, M. A. A Recyclable, Immobilized Analogue of Benzotetramisole for Catalytic Enantioselective Domino Michael Addition/Cyclization Reactions in Batch and Flow. *ACS Catal.* **2016**, *6* (1), 348−356.
(22) Moore, L. C.; Lo, A.; Fell, J. S.; Duong, M. R.; Moreno, J. A.; Rich, B. E.; Bravo, M.; Fettinger, J. C.; Souza, L. W.; Olmstead, M. M.; Houk, K. N.; Shaw, J. T. Acyclic Stereocontrol in the Additions of Nucleophilic Alkenes to A-Chiral *N* -Sulfonyl Imines. *Chem. - Eur. J.* **2019**, *25* (52), 12214−12220.
(23) Stubbing, L. A.; Savage, G. P.; Brimble, M. A. N-Alkylsulfonylimines as Dipolarophiles in Cycloaddition Reactions. *Chem. - Asian J.* **2013**, *8*, 42−48.
(24) Luo, Y.; Hepburn, H. B.; Chotsaeng, N.; Lam, H. W. Enantioselective Rhodium-Catalyzed Nucleophilic Allylation of Cyclic Imines with Allylboron Reagents. *Angew. Chem., Int. Ed.* **2012**, *51* (33), 8309−8313.
(25) Xiong, X. F.; Zhang, H.; Peng, J.; Chen, Y. C. Direct Asymmetric Michael Addition of Cyclic N-Sulfonylimines to α,β-Unsaturated Aldehydes. *Chem. - Eur. J.* **2011**, *17* (8), 2358−2360.
(26) Laha, J. K.; Jethava, K. P. Access to Imidazolidine-Fused Sulfamidates and Sulfamides Bearing a Quaternary Center via 1,3-Dipolar Cycloaddition of Nonstabilized Azomethine Ylides. *J. Org. Chem.* **2017**, *82* (7), 3597−3604.
(27) Laha, J. K.; Jethava, K. P.; Tummalapalli, K. S. S.; Sharma, S. Synthesis of Mono-N-Sulfonylimidazolidines by a 1,3-Dipolar Cycloaddition Strategy, as an Alternative to Selective N-Sulfonylation, and Their Ring Cleavage To Afford 1,2-Diamines. *Eur. J. Org. Chem.* **2017**, *2017* (31), 4617−4624.
(28) Hu, P.; Hu, J.; Jiao, J.; Tong, X. Amine-Promoted Asymmetric (4 + 2) Annulations for the Enantioselective Synthesis of Tetrahydropyridines: A Traceless and Recoverable Auxiliary Strategy. *Angew. Chem., Int. Ed.* **2013**, *52* (20), 5319−5322.
(29) Kravina, A. G.; Mahatthananchai, J.; Bode, J. W. Enantioselective, NHC-Catalyzed Annulations of Trisubstituted Enals and Cyclic n-Sulfonylimines via α,β-Unsaturated Acyl Azoliums. *Angew. Chem., Int. Ed.* **2012**, *51* (37), 9433−9436.
(30) Chen, X. Y.; Lin, R. C.; Ye, S. Catalytic [2 + 2] and [3 + 2] Cycloaddition Reactions of Allenoates with Cyclic Ketimines. *Chem. Commun.* **2012**, *48* (9), 1317−1319.
(31) Spielmann, K.; Van Der Lee, A.; De Figueiredo, R. M.; Campagne, J. M. Diastereoselective Palladium-Catalyzed (3 + 2)-Cycloadditions from Cyclic Imines and Vinyl Aziridines. *Org. Lett.* **2018**, *20* (5), 1444−1447.
(32) Nishimura, T.; Noishiki, A.; Chit Tsui, G.; Hayashi, T. Asymmetric Synthesis of (Triaryl)Methylamines by Rhodium-Catalyzed Addition of Arylboroxines to Cyclic N-Sulfonyl Ketimines. *J. Am. Chem. Soc.* **2012**, *134* (11), 5056−5059.
(33) Wang, H.; Jiang, T.; Xu, M. H. Simple Branched Sulfur-Olefins as Chiral Ligands for Rh-Catalyzed Asymmetric Arylation of Cyclic Ketimines: Highly Enantioselective Construction of Tetrasubstituted Carbon Stereocenters. *J. Am. Chem. Soc.* **2013**, *135* (3), 971−974.
(34) Li, Y.; Yu, Y. N.; Xu, M. H. Simple Open-Chain Phosphite-Olefin as Ligand for Rh-Catalyzed Asymmetric Arylation of Cyclic Ketimines: Enantioselective Access to Gem-Diaryl α-Amino Acid Derivatives. *ACS Catal.* **2016**, *6* (2), 661−665.
(35) De Munck, L.; Monleón, A.; Vila, C.; Pedro, J. R. Diarylprolinol as a Ligand for Enantioselective Alkynylation of Cyclic Imines. *Adv. Synth. Catal.* **2017**, *359* (9), 1582−1587.
(36) Huang, Y.; Huang, R. Z.; Zhao, Y. Cobalt-Catalyzed Enantioselective Vinylation of Activated Ketones and Imines. *J. Am. Chem. Soc.* **2016**, *138* (20), 6571−6576.
(37) Quan, M.; Wang, X.; Wu, L.; Gridnev, I. D.; Yang, G.; Zhang, W. Ni(II)-Catalyzed Asymmetric Alkenylations of Ketimines. *Nat. Commun.* **2018**, *9* (1), 2258.
(38) Vaidya, A.; Jain, S.; Jain, P.; Jain, P.; Tiwari, N.; Jain, R.; Jain, R.; K. Jain, A.; K. Agrawal, R. Synthesis and Biological Activities of Oxadiazole Derivatives: A Review. *Mini-Rev. Med. Chem.* **2016**, *16*, 825−845.
(39) Khalilullah, H.; J. Ahsan, M.; Hedaitullah, M.; Khan, S.; Ahmed, B. 1,3,4-Oxadiazole: A Biologically Active Scaffold. *Mini-Rev. Med. Chem.* **2012**, *12* (8), 789−801.

https://dx.doi.org/10.1021/acs.orglett.0c03083
Org. Lett. XXXX, XXX, XXX−XXX

(40) Verma, G.; Khan, M. F.; Akhtar, W.; Alam, M. M.; Akhter, M.; Shaquiquzzaman, M. A Review Exploring Therapeutic Worth of 1,3,4-Oxadiazole Tailored Compounds. *Mini-Rev. Med. Chem.* **2019**, *19* (6), 477−509.
(41) Katritzky, A. R.; Rees, C. W. *Comprehensive Heterocyclic Chemistry*; Elsevier, 2009; Vols. *1*−*7*.
(42) Slobbe, P.; Ruijter, E.; Orru, R. V. A. Recent Applications of Multicomponent Reactions in Medicinal Chemistry. *MedChemComm* **2012**, *3*, 1189−1218.
(43) Rotstein, B. H.; Zaretsky, S.; Rai, V.; Yudin, A. K. Small Heterocycles in Multicomponent Reactions. *Chem. Rev.* **2014**, *114*, 8323−8359.
(44) Dömling, A.; Wang, W.; Wang, K. Chemistry and Biology of Multicomponent Reactions. *Chem. Rev.* **2012**, *112*, 3083−3135.
(45) Saiz, C.; Wipf, P.; Manta, E.; Mahler, G. Reversible Thiazolidine Exchange: A New Reaction Suitable for Dynamic Combinatorial Chemistry. *Org. Lett.* **2009**, *11* (15), 3170−3173.
(46) Maskrey, T. S.; Frischling, M. C.; Rice, M. L.; Wipf, P. A Five-Component Biginelli-Diels-Alder Cascade Reaction. *Front. Chem.* **2018**, *6*, 376.
(47) Ramazani, A.; Rezaei, A. Novel One-Pot, Four-Component Condensation Reaction: An Efficient Approach for the Synthesis of 2,5-Disubstituted 1,3,4-Oxadiazole Derivatives by a Ugi-4CR/Aza-Wittig Sequence. *Org. Lett.* **2010**, *12* (12), 2852−2855.
(48) Appavoo, S. D.; Kaji, T.; Frost, J. R.; Scully, C. C. G.; Yudin, A. K. Development of Endocyclic Control Elements for Peptide Macrocycles. *J. Am. Chem. Soc.* **2018**, *140* (28), 8763−8770.
(49) Frost, J. R.; Scully, C. C. G.; Yudin, A. K. Oxadiazole Grafts in Peptide Macrocycles. *Nat. Chem.* **2016**, *8* (12), 1105−1111.
(50) Belowich, M. E.; Stoddart, J. F. Dynamic Imine Chemistry. *Chem. Soc. Rev.* **2012**, *41*, 2003−2024.
(51) Wang, Q.; Mgimpatsang, K. C.; Konstantinidou, M.; Shishkina, S. V.; Dömling, A. 1,3,4-Oxadiazoles by Ugi-Tetrazole and Huisgen Reaction. *Org. Lett.* **2019**, *21* (18), 7320−7323.
(52) Contreras, R. R.; Fuentealba, P.; Galván, M.; Pérez, P. A Direct Evaluation of Regional Fukui Functions in Molecules. *Chem. Phys. Lett.* **1999**, *304* (5−6), 405−413.
(53) Chang, D. J.; Jeong, M. Y.; Song, J.; Jin, C. Y.; Suh, Y. G.; Kim, H. J.; Min, K. H. Discovery of Small Molecules That Enhance Astrocyte Differentiation in Rat Fetal Neural Stem Cells. *Bioorg. Med. Chem. Lett.* **2011**, *21* (23), 7050−7053.
(54) Quinlan, J. R. Induction of Decision Trees. *Machine Learning* **1986**, *1* (1), 81−106.
(55) Rogers, D.; Hahn, M. Extended-Connectivity Fingerprints. *J. Chem. Inf. Model.* **2010**, *50* (5), 742−754.
(56) Cohen, J. Weighted Kappa: Nominal Scale Agreement Provision for Scaled Disagreement or Partial Credit. *Psychol. Bull.* **1968**, *70* (4), 213−220.
(57) McHugh, M. L. Interrater Reliability: The Kappa Statistic. *Biochem. Medica* **2012**, *22* (3), 276−282.
(58) Jethava, K. P.; Fine, J. A.; Chen, Y.; Hossain, A.; Chopra, G. Accelerated Reactivity Mechanism and Interpretable Machine Learning Model of N-Sulfonylimines Towards Fast Multicomponent Reactions. *ChemRxiv* **2020**, DOI: 10.26434/CHEMRXIV.12116163.V1.

https://dx.doi.org/10.1021/acs.orglett.0c03083
Org. Lett. XXXX, XXX, XXX−XXX